Homometallic ferrimagnetism in the zig-zag chain compound $Na_2Cu_5Si_4O_{14}$

M. S. Reis,* A. Moreira dos Santos, and V. S. Amaral
Departamento de Física and CICECO, Universidade de Aveiro, 3810-193 Aveiro, Portugal

P. Brandão and J. Rocha
Departamento de Química and CICECO, Universidade de Aveiro, 3810-193 Aveiro, Portugal
(Received 31 January 2006; revised manuscript received 9 March 2006; published 8 June 2006)

The structure of $Na_2Cu_5Si_4O_{14}$ is comprised of zig-zag chains of alternating Cu edge-sharing dimers and trimers, with different magnetic ground states, allowing the occurrence of homometallic ferrimagnetism. The magnetic susceptibility data are consistent with that of a ferrimagnetic chain compound, and are predicted using a model that considers interactions intra-trimers (related to the exchange integral $J_1=-224.9$ K), intra-dimer ($J_3=40.22$ K), and inter dimer-trimer ($J_2=-8.01$ K). The magnetic interaction between the antiferromagnetic trimer and ferromagnetic dimer is in accordance with the Goodenough rules applied to the Cu-O topology. A three-dimensional antiferromagnetic ordering is observed below $T_N=8$ K, corresponding to the magnetic ordering between chains. In addition, since $T_N \sim \theta_p$ there is not a significant degree of frustration in the chain ordering.

DOI: 10.1103/PhysRevB.73.214415 PACS number(s): 75.10.Pq, 75.30.Et, 75.50.Xx

I. INTRODUCTION

Low-dimensional magnetism has attracted a great deal of attention in recent years. Zero-dimensional (isolated molecule) and one-dimensional (1D) (chain) systems can exhibit a great variety of exotic magnetic behavior, from superparamagnetism to Spin-Peierls transitions[1] and Haldane chains,[2–4] among others. In most instances, materials exhibiting low-dimensional behavior are metalorganic compounds. Examples include molecular magnets and coordination polymers, which derive their magnetic character directly from the topology of the metalorganic framework, while the relatively large organic ligands work as spacers, between the magnetically active centers, preserving the low-dimensionality behavior even at low temperatures.[5,6] On the other hand, crystalline inorganic systems exhibiting magnetic clusters or chains are rare, mainly because, in most instances, their structure has a pronounced three-dimensional (3D) character and, even when that is not the case, the interaction between magnetic centers hampers the clear observation of low dimensionality of magnetic order before the onset of the three-dimensional order. Notable exceptions of this are the Spin-Peierls $CuGeO_3$, the first observation of such a behavior in an inorganic system,[1] the Haldane chain compound Y_2NiBaO_5,[2–4] Cu triangles[7] as in $La_4Cu_3MoO_{12}$, ladders[8] in $Sr_{14}Cu_{24}O_{41}$, and dimer chains in $Na_2Cu_2Si_4O_{11}$.[9] New advances in synthetic inorganic chemistry, such as sol gel, hydrothermal synthesis, or pillaring reactions, for instance, have been providing a wealth of new compounds, often metastable, and usually unaccessible from traditional high-temperature methods, which adds powerful tools for the design of new inorganic materials with interesting topology and properties. In particular, the incorporation of magnetic ions in the starting reaction gel can afford these systems with interesting magnetic properties.[10] Despite their scarcity, low-dimensionality inorganic systems are of interest not only due to their higher chemical and mechanical stability but also because they are more amenable to integration in more complex electromagnetic devices.[11]

Although antiferromagnetism is by far the most common type of magnetic ordering, systems with finite magnetization in the ground state (ferro or ferrimagnetism) are considered more useful for technical applications, such as quantum computing, spin polarization, and data storage. Ferrimagnetism, for instance, can easily be achieved in bimetallic systems through an antiparallel coupling of ions with different spin values, yielding a remanescent magnetization.[12] The mechanism for homometallic ferrimagnetism, however, is often more subtle.[13] The two mechanisms that can cause such behavior are either an alternation of the g-factor as observed in Co_2-EDTA,[14] or a topology including odd numbers of metal centers with complex magnetic exchange interactions, as observed in $A_3Cu_3(PO_4)_4$ (A=Ca, Sr), where Cu linear trimers interact with each other resulting in ferrimagnetism.[15] Here, we wish to report on a ferrimagnetic homometallic sodium copper silicate that exhibits parallel zig-zag chains comprised of trimers and dimers of edge-sharing square-planar CuO_4. We have accounted for its magnetization behavior using a spin Hamiltonian, comprised of dimer and trimer terms together with a pseudo-1D interaction.

II. MATERIAL DETAILS

A. Sample preparation procedure

The synthesis of $Na_2Cu_5Si_4O_{14}$ was carried out in teflon-lined autoclave under static hydrothermal conditions. Typically, an alkaline solution was made by mixing 6.86 g of sodium silicate solution (Na_2O 8 wt % and SiO_2 27 wt %, Merck), 7.37 g of H_2O, and 2.25 g of NaOH (Panreac). A second solution was made by mixing 8.97 g of H_2O with 1.80 g of $CuSO_4 \cdot 5H_2O$ (Pronalab). These two solutions were combined and stirred thoroughly for 1 h. The gel with a composition $5.14Na_2O:CuO:4.28SiO_2:126.08H_2O$ was autoclaved for 7 days at 230 °C. The crystalline powder was filtered off, washed, and dried at 50 °C overnight. The crystal structure of the compound was determined through syn-

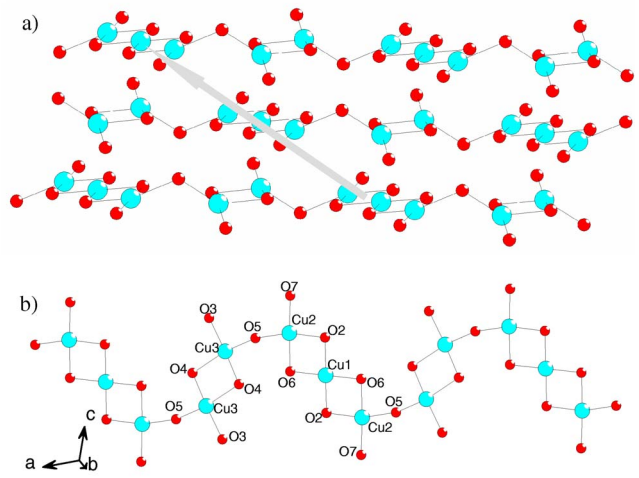

FIG. 1. (Color online) The structure of the Cu–O zig-zag chain. (a) The arrow indicates the staggered stacking of the chains. (b) Top view of the chain, note the alternation of the dimer and trimer units, connected by O_5.

chrotron radiation powder diffraction. Details of the synthesis, as well as the structure determination methods and crystal data, will be published elsewhere. Magnetic susceptibility χ ($=M/H$ at low magnetic field) was measured on a powder sample using a conventional superconducting quantum interference device (SQUID) magnetometer, between 5 and 300 K.

B. Crystal structure

The compound $Na_2Cu_5Si_4O_{14}$, structurally similar to $Li_2Cu_5Si_4O_{14}$,[16] contains Si_2O_7 double tetrahedra, characteristic of the sorosilicate mineral family. The metal–oxygen connectivity consists of zig-zag chains of edge-sharing square-planar CuO_4. These chains are stacked obliquely in adjacent planes, as seen in Fig. 1(a), and are separated in the plane by the double tetrahedra and the sodium ion (not shown). Each link of the chain is an alternating edge-sharing Cu_2O_6 dimer and Cu_3O_8 trimer connected by their corners. A top view of a single chain is shown in Fig. 1(b), and the relevant structural data are listed in Table I. Although the coordination of the Cu ions is square planar, it should be noticed that each end of the trimer has an O ion lying apically, in a pseudo-square pyramidal-like coordination, but too distant to be part of a Cu Jahn-Teller distortion compounds (usually, the apical Cu-O distance is up to 2.75 Å). A zig-zag chain with two types of building blocks is quite unusual: Although dimers, trimers, and chain systems have been studied in detail, both from the theoretical and experimental side (see, for example, the book by Khan),[17] this is a magnetic study of a compound that simultaneously exhibits these three characters (dimer, trimer, and chain) in its structure.

C. Magnetic behavior

The variation of the magnetic susceptibility χ as a function of temperature with an applied field of 100 Oe was measured, and is shown in Fig. 2(a). It shows a monotonic increase of susceptibility down to 8 K, where a sharp drop indicates a possible 3D ground state. At temperatures in the range of 8–100 K, the susceptibility exceeds what would be expected from the extrapolation of the paramagnetic Curie-Weiss region (see the right-hand side axis), indicating that in the low-temperature regime, there is no spin cancellation.

In Fig. 2(b), χT versus temperature is shown. The plot shows a broad minimum at 64 K, increasing to a maximum at 36 K before a sharp decrease to the ground state. These features have been reported in the literature for one-

TABLE I. Selected structural parameters for the Cu–O chain.

Bond lengths		Bond angles	
Cu_1-O_2	1.949 Å	$Cu_1-O_2-Cu_2$	100.18°
Cu_2-O_2	1.966 Å	$Cu_1-O_6-Cu_2$	100.65°
Cu_2-O_7 $(2-x,2-y,-z)$	2.707 Å (apical)	$Cu_3-O_4-Cu_3$	97.22°
Cu_2-O_6	1.951 Å	$Cu_2-O_5-Cu_3$	119.56°
Cu_3-O_4	1.921 Å		
Cu_3-O_3	1.891 Å		
Cu_1-O_6	1.950 Å		
Cu_2-O_5	1.982 Å		
Cu_2-O_7	1.919 Å		
Cu_3-O_4	1.979 Å		
Cu_3-O_5	1.958 Å		

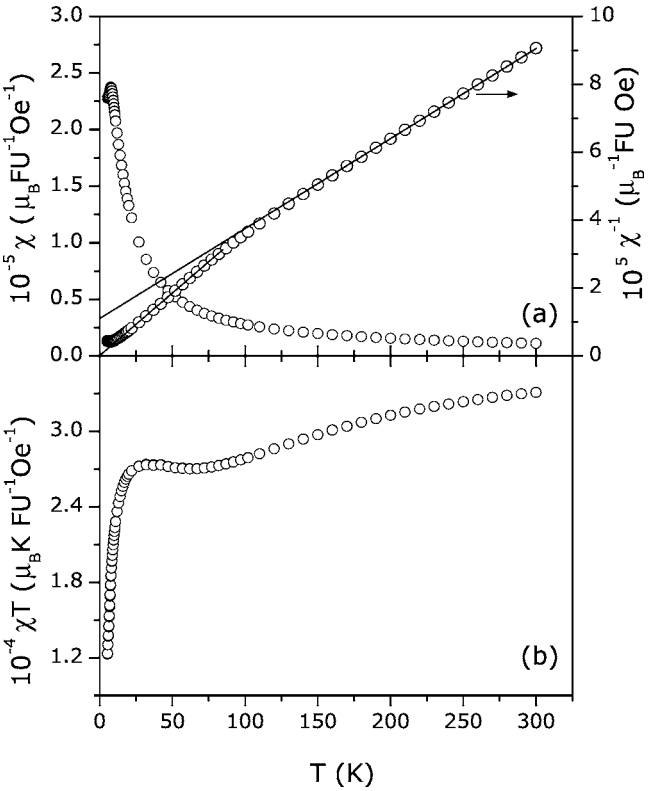

FIG. 2. Measured magnetic susceptibility, its inverse, and χT as a function of temperature. The straight line is an extrapolation from the high-temperature regime.

dimensional compounds, where this broad minimum is associated with 1D ferrimagnetism.[6,13,18,19] The sharp decrease in the plot at low temperatures is sometimes associated with a transition to the 3D antiferromagnetic state,[20] while a divergence to higher values would be interpreted as a ferrimagnetic ground state.[15] However, from our model—developed and explained in the next section—we conclude that both those signatures can be consistent with ferrimagnetism. Therefore, the ferrimagnetic behavior dominates the susceptibility curve down to the observed onset of 3D ordering (8 K). In fact, the type of divergence upon cooling seems highly correlated with structural effects. Indeed, there are several instances where a change in the atomic species may result in two types of behavior, for example, in $CuX_2 \cdot TMSO$ (X=Br, Cl) (Ref. 20) and $A_3Cu_3(PO_4)_4$ (A=Ca, Sr).[13]

III. THEORETICAL PICTURE

As described above, the structure obtained for $Na_2Cu_5Si_4O_{14}$, in conjunction with the observed susceptibility data, suggests that the strongest magnetic interaction lies along the dimer-trimer chain. However, as a first approximation, that allows the exact solution of the Hamiltonian, we will consider a dimer-trimer cluster, with local 1D signatures. Later, this assumption will be discussed in detail. Therefore, let us consider the following Hamiltonian, written in accordance with Fig. 3:

$$\mathcal{H} = -J_1(S_1S_2 + S_2S_3) - J_2S_AS_B - J_3S_4S_5 - g\mu_BHS, \quad (1)$$

where $S_B=S_1+S_2+S_3$, $S_A=S_4+S_5$, and $S=S_A+S_B$ correspond to the total spin of the dimer-trimer pair. Let us also define $S_{B'}=S_1+S_3$, and rewrite Eq. (1) in the following way:

$$\mathcal{H} = -\frac{J_1}{2}(S_B^2 - S_{B'}^2 - S_2^2) - \frac{J_2}{2}(S^2 - S_A^2 - S_B^2) - \frac{J_3}{2}(S_A^2 - S_4^2 - S_5^2) - g\mu_BHS. \quad (2)$$

Changing the zero of energy, the eigenvalues of the previous Hamiltonian are:

$$E_\Omega = -\frac{J_1}{2}[s_B(s_B+1) - s_{B'}(s_{B'}+1)] - \frac{J_2}{2}[s(s+1) - s_A(s_A+1) - s_B(s_B+1)] - \frac{J_3}{2}[s_A(s_A+1)] - g\mu_BHm_S, \quad (3)$$

where

$$\Omega \rightarrow \begin{cases} |5/2,1,3/2,1\rangle \\ |3/2,1,1/2,1\rangle \\ |3/2,1,1/2,0\rangle \\ |3/2,0,3/2,1\rangle \\ |1/2,0,1/2,1\rangle \\ |1/2,0,1/2,0\rangle \\ |1/2,1,3/2,1\rangle \\ |1/2,1,1/2,1\rangle \\ |1/2,1,1/2,0\rangle \end{cases} \quad (4)$$

represents each state allowed by the system in the basis $|s,s_A,s_B,s_{B'}\rangle$.

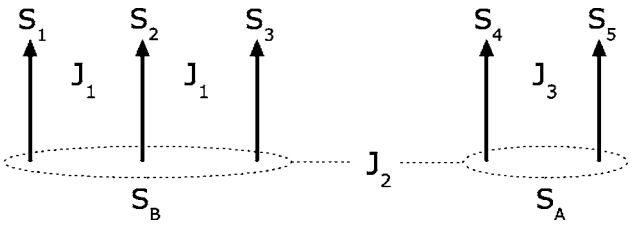

FIG. 3. Schematic view of the dimer-trimer cluster, with the respective exchange interactions: J_1-intra-trimer, J_3-intra-dimer, and J_2-inter trimer-dimer.

The magnetization of the system can be derived from the following equation:

$$\mathcal{M} = g\mu_B \frac{\Sigma_\Omega(\Sigma_{m_s} m_s e^{\bar{x}m_s}) e^{-E_\Omega^{(0)}/kT}}{\Sigma_\Omega(\Sigma_{m_s} e^{\bar{x}m_s}) e^{-E_\Omega^{(0)}/kT}}(4), \quad (5)$$

where

$$\bar{x} = \frac{g\mu_BH}{kT} \quad (6)$$

and $E_\Omega^{(0)}=E_\Omega(H=0)$ represent the zero-field eigenvalues of the energy:

$$E_\Omega^{(0)} = -\frac{1}{2}\begin{pmatrix} 7/4 & 3 & 2 \\ -5/4 & 1 & 2 \\ 3/4 & 1 & 2 \\ 7/4 & 0 & 0 \\ -5/4 & 0 & 0 \\ 3/4 & 0 & 0 \\ 7/4 & -5 & 2 \\ -5/4 & -2 & 2 \\ 3/4 & -2 & 2 \end{pmatrix} \cdot \begin{pmatrix} J_1 \\ J_2 \\ J_3 \end{pmatrix}. \quad (7)$$

Let us now suppose that there are no interactions between clusters. The paramagnetic susceptibility may be obtained from Eq. (5):

$$\chi_p = \frac{C'}{T}, \quad (8)$$

where

$$C' = C'(T) = \frac{(g\mu_B)^2}{3k} \frac{\Sigma_\Omega l_\Omega e^{-E_\Omega^{(0)}/kT}}{\Sigma_\Omega k_\Omega e^{-E_\Omega^{(0)}/kT}} \quad (9)$$

with $l_\Omega=s(s+1)(2s+1)$ and $k_\Omega=(2s+1)$.

From Eq. (8), it is possible to obtain the high-temperature limit:

$$\gamma\chi_pT = \frac{\Sigma_\Omega l_\Omega}{\Sigma_\Omega k_\Omega} = 5s_n(s_n+1), \quad (10)$$

where $\gamma=3k/(g\mu_B)^2$ and s_n is the spin of a free Cu^{2+} ion, i.e., $s_n=1/2$. On the other hand, the low-temperature limit can also be derived:

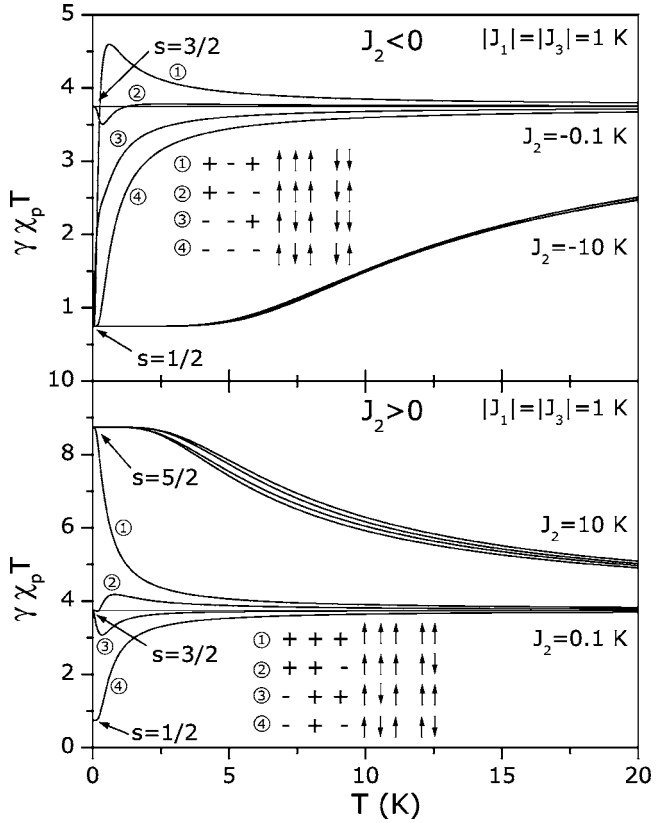

FIG. 4. Behavior of $\gamma\chi_p T$ as a function of temperature for several combinations of exchange interactions J_1, J_2, and J_3. The four sets of three + and − correspond, respectively, to the sign of those magnetic interactions (J_1, J_2, and J_3). Each set is related to one curve in the respective order, from the top to the bottom.

$$\gamma\chi_p T = s(s+1), \tag{11}$$

where, s represents the total spin of the ground state configuration of the trimer-dimer pair. Therefore, $\gamma\chi_p T$, as a function of temperature, can present different behaviors with, at low temperatures, a positive (or negative) derivative if $s(s+1)$ is smaller (larger) than $5s_n(s_n+1)$. These features are illustrated in Fig. 4 for several combinations of the exchange interactions J_1, J_2, and J_3. For example, Curve 1 of Fig. 4 (bottom) has a ferromagnetic ground state and, however, has a strong and negative derivative at low temperatures. In addition, several curves of Fig. 4 present a positive derivative at low temperatures and, in spite of this, still correspond to a 1D ferrimagnetic system in that temperature range. These theoretical results shed some light on some previous reports that made erroneous interpretations of the low-temperature magnetic data, regarding the claim that the onset of antiferromagnetism occurs when the derivative of the susceptibility turns positive (increasing χT with increasing temperature).[13,19]

IV. CONNECTIONS WITH EXPERIMENTAL RESULTS

From the model developed and presented in Sec. III, we predict and trace the experimental magnetic susceptibility presented in Fig. 2, considering Eq. (8) with a residual temperature independent diamagnetic contribution χ_d, i.e.,

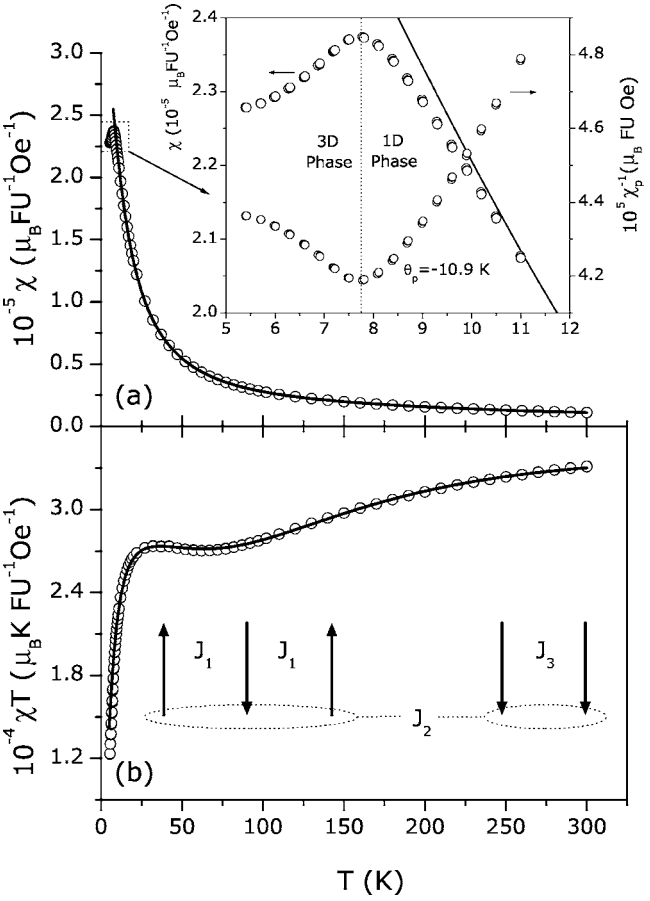

FIG. 5. Experimental (open circles) and theoretical [solid line—Eq. (12)] (a) magnetic susceptibilities and (b) magnetic susceptibilities multiplied by temperature. The inset in (a) emphasizes the 1D-3D transition found in this material. The diagram in (b) represents the ground-state arrangement of the spins, following the obtained free parameters.

$$\chi(T) = \chi_p(T) + \chi_d. \tag{12}$$

Equation (12) was fitted to the experimental data using a least-squares minimization procedure, yielding the parameters: $J_1 = -224.90$ K, $J_2 = -8.01$ K, $J_3 = 40.22$ K, $g = 2.30$, and $\chi_d = -1.33 \times 10^{-7} \mu_B$ FU^{-1} Oe^{-1}, as presented in Fig. 5. That value of g was already found in another Cu^{2+} compound.[15] These values clarify the ground state of the spin arrangement, where the dimer aligns ferromagnetically, the trimer antiferromagnetically and, finally, the net spin of the dimer and trimer, i.e., S_A and S_B, respectively, have an antiparallel alignment, as shown in Fig. 5(b). The signs of the magnetic exchange interaction for the trimer (antiferromagnetic) and dimer (ferromagnetic) are in agreement with the Goodenough-Kanamori[21] rules, that correlate the type of interaction with the cation-anion-cation bond angle. It is predicted that, as the angle increases from 90°, there should be a crossover from ferromagnetism to antiferromagnetism. A recent review of Cu compounds,[22] suggests that for edge-sharing Cu_2O_2 units, the crossover angle is 97°, although the exact value can vary due to influence of other neighboring

structural elements. In Table I, it can be seen that all $Cu_{trimer}-O-Cu_{trimer}$ angles fall well in the antiferromagnetic regime, while the $Cu_{dimer}-O-Cu_{dimer}$ angle is very close to the ferromagnetic range.

From the fitting parameters, we concluded that the magnetic susceptibility at higher temperature, is ruled by the intratrimer interactions (via $J_1=-224.90$ K). At intermediate values, the intra-dimer interactions (via $J_3=40.22$ K), start to become perceptible along with the intra-trimer interactions. Finally, the interactions between dimers and trimers work only at low values of temperature, comparable to the value of $J_2=-8.01$ K, which is quite close to the onset temperature of the 3D order (8 K). Thus, the rich magnetic susceptibility behavior found for this material (from room temperature down to 8 K) is exclusively due to the internal degrees of freedom of dimers and trimers; and differences between chain and clusters models would be significant only below 8 K, when the 3D order steps in. In other words, the interactions between dimers and trimers are overwhelmed by the 3D order, justifying the use of a cluster model.

Figure 5(a) shows the magnetic susceptibility, with special attention given to the low-temperature region, emphasizing the transition from the 1D to the 3D phase. The inverse paramagnetic susceptibility (discounting the diamagnetic contribution) is presented on the right-hand side axis of the inset of Fig. 5(a). An extrapolation of this quantity gives $\theta_p=-10.9$ K. This result shows that the long-range magnetic order (3D phase) has an antiferromagnetic character, and the critical temperature T_c is, strictly speaking, a Neel temperature T_N. In other words, the spin chains are in an antiparallel alignment. In addition, since $T_N \sim \theta_p$, there is not a significant degree of frustration in the chain ordering. A further and thorough analysis of the low-temperature regime (3D phase), will be published elsewhere.

From the obtained free parameters and using Eq. (5), we evaluated the magnetization of the system. Due to the quite weak magnetic interaction between the dimer and trimer, i.e., between S_A and S_B, via $J_2=-8.01$ K, the magnetization, for measurable values of temperature (around 50 K), does not present a plateau at $s=1/2$, since the external magnetic field easily aligns the dimer with respect to the net spin S_B of the trimer. Thus, the first magnetic saturation lies in $s=3/2$ ($s_A=1$ and $s_B=1/2$). A further increase in the external magnetic field flips the spin of the trimer ($s_B: 1/2 \rightarrow 3/2$); however, only for magnetic fields larger than 3×10^2 T, due to the strong intra-trimer magnetic interaction ($J_1=-224.90$ K). These features are presented in the inset of Fig. 6, where the arrows represent the dimer-trimer pair and its most probable arrangement, depending on the value of applied magnetic field.

In this direction, we measured some $M(H)$ curves up to 5 T in the paramagnetic phase, and could not find any magnetization plateau, corroborating the prediction that at those temperatures the magnetic saturation is quite far from the standard 5 T, as presented in Fig. 6. The open circles represent the experimental data; and the full line the magnetization, obtained from Eq. (5) and those values from the susceptibility analysis (Fig. 5). Note that the full line is not a fit to the data and works better in the susceptibility regime, as expected.

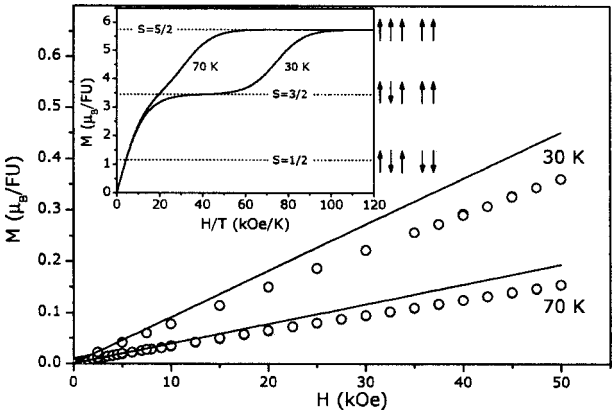

FIG. 6. Inset: Predicted magnetization, using Eq. (5) and those values obtained from the analysis of the magnetic susceptibility, presented in Fig. 5. Lower values of the magnetic field can flip the dimer, due to the weak inter trimer-dimer exchange interaction $J_2=-8.01$ K. On the other hand, only very large values of magnetic field are strong enough to break the strong antiferromagnetic order of the trimer, represented by $J_1=-224.90$ K. Those sets of arrows represent the dimer-trimer pair and its most probable arrangement, depending on the value of applied magnetic field. Main graphic: Open circles represent the experimental data, whereas the full line is the predicted magnetization, obtained from Eq. (5) and also using the values obtained from the analysis of the magnetic susceptibility.

V. CONCLUDING REMARKS

We reported a ferrimagnetic homometallic sodium copper silicate $Na_2Cu_5Si_4O_{14}$ that exhibits parallel staggered zig-zag chains with alternating trimers and dimers, originating a ferrimagnetic arrangement in the chain. From the model developed, we concluded that the exotic magnetic susceptibility found for this material (from room temperature down to 8 K) is exclusively due to the internal degrees of freedom of dimers and trimers. At low temperatures, below 8 K, a long-range magnetic order steps in, establishing a 3D order, with an interchain antiferromagnetic arrangement, without frustration in the ground state, since $T_N \sim \theta_p$. Finally, our results shows that the reduction of the χT quantity, with decreasing temperature, can be consistent with a ferrimagnetic ground state within chains.

ACKNOWLEDGMENT

The authors are thankful to A. M. Gomes and A. Fitch, for some magnetic and powder synchrotron measurements, respectively. Two of the authors (A.M.S. and M.S.R.) acknowledge the FCT Grant Nos. BPD/14984/2004 and BPD/23184/2005, respectively. Funding for the work was provided by a FCT grant (No. CTM/46780).

*Electronic address: marior@fis.ua.pt

[1] M. Hase, I. Terasaki, and K. Uchinokura, Phys. Rev. Lett. **70**, 3651 (1993).
[2] J. Darriet and L. P. Regnault, Solid State Commun. **86**, 409 (1993).
[3] J. F. DiTusa, S. W. Cheong, C. Broholm, G. Aeppli, L. W. Rupp, and B. Batlogg, Physica B **181**, 194 (1994).
[4] J. F. DiTusa, S. W. Cheong, J. H. Park, G. Aeppli, G. Broholm, and C. T. Chen, Phys. Rev. Lett. **73**, 1857 (1994).
[5] M. Verdaguer, Polyhedron **20**, 1115 (2001).
[6] S. J. Blundell and F. L. Pratt, J. Phys.: Condens. Matter **16**, R771 (2004).
[7] M. Azuma, T. Odaka, M. Takano, D. A. Vander-Griend, K. R. Poeppelmeier, Y. Narumi, K. Kindo, Y. Mizuno, and S. Maekawa, Phys. Rev. B **62**, R3588 (2000).
[8] R. S. Eccleston, M. Uehara, J. Akimitsu, H. Eisaki, N. Motoyama, and S. Uchida, Phys. Rev. Lett. **81**, 1702 (1998).
[9] A. M. dos Santos, V. S. Amaral, P. Brandão, F. A. A. Paz, J. Rocha, L. P. Ferreira, M. Godinho, O. Volkova, and A. Vasiliev, Phys. Rev. B **72**, 092403 (2005).
[10] A. B. Bourlinos, R. Zboril, and D. Petridis, Microporous Mesoporous Mater. **58**, 155 (2003).
[11] S. Jing, M. K. James, P. Roger, S. Tilman, D. A. David, M. R. Gilberto, and P. M. Petroff, Nature (London) **377**, 707 (1995).
[12] E. Coronada, M. Drillon, P. R. Nugteren, L. J. Dejongh, D. Beltran, and R. Georges, J. Am. Chem. Soc. **111**, 3874 (1989).
[13] M. A. M. Abu-Youssef, A. Escuer, M. A. S. Goher, F. A. Mautner, G. J. Reiss, and R. Vicente, Angew. Chem., Int. Ed. **39**, 1624 (2000).
[14] E. Coronada, M. Drillon, P. R. Nugteren, L. J. Dejongh, D. Beltran, and R. Georges, J. Am. Chem. Soc. **110**, 3907 (1988).
[15] A. A. Belik, A. Matsuo, M. Azuma, K. Kindo, and M. Takano, J. Solid State Chem. **178**, 709 (2005).
[16] K. Kawamura, A. Kawahara, and J. Iiyama, Acta Crystallogr. **34**, 3181 (1978).
[17] O. Kahn, *Molecular Magnetism* (Wiley-VCH, New-York, 1993).
[18] E. Coronado, C. J. Gomezgarcia, and J. J. Borrasalmanar, J. Appl. Phys. **67**, 6009 (1990).
[19] M. Drillon, E. Coronado, M. Belaiche, and R. L. Carlin, J. Appl. Phys. **63**, 3551 (1988).
[20] C. P. Landee, A. Djili, D. F. Mudgett, M. Newhall, H. Place, B. Scott, and R. Willet, Inorg. Chem. **27**, 620 (1988).
[21] J. B. Goodenough, Phys. Rev. **100**, 564 (1955).
[22] G. V. R. Chandramouli, T. K. Kundu, and P. T. Manoharan, Aust. J. Chem. **56**, 1239 (2003).